International Journal of Heat and Fluid Flow 30 (2009) 131–139

Contents lists available at ScienceDirect

International Journal of Heat and Fluid Flow

journal homepage: www.elsevier.com/locate/ijhff

Frictional pressure drop during vapour–liquid flow in minichannels: Modelling and experimental evaluation

A. Cavallini, D. Del Col, M. Matkovic, L. Rossetto *

Università di Padova, Dipartimento di Fisica Tecnica, Via Venezia 1, 35131 Padova, Italy

ARTICLE INFO

Article history:
Received 28 July 2007
Received in revised form 18 February 2008
Accepted 12 September 2008
Available online 14 November 2008

Keywords:
Minichannel
Pressure drop
Single phase
Two phase
Entrainment
Roughness

ABSTRACT

Condensation in minichannels is widely used in air-cooled condensers for the automotive and air-conditioning industry, in heat pipes and other applications for system thermal control. The knowledge of pressure drops in such small channels is important in order to optimize heat transfer surfaces. This paper presents a model for calculation of the frictional pressure gradient during condensation or adiabatic liquid–gas flow inside minichannels with different surface roughness. In order to account for the effects of surface roughness, new experimental frictional pressure gradient data associated to single-phase flow and adiabatic two-phase flow of R134a inside a single horizontal mini tube with rough wall has been used in the modelling. It is a Friedel (1979) [Friedel, L., 1979. Improved friction pressure drop correlations for horizontal and vertical two-phase pipe flow. In: Proceedings of the European Two-Phase Flow Group Meeting, Ispra, Paper E2] based model and it takes into account mass velocity, vapor quality, fluid properties, reduced pressure, tube diameter, entrainment ratio and surface roughness. With respect to the flow pattern prediction capability, it has been built for shear dominated flow regimes inside pipes, thus, annular, annular-mist and mist flow are here predicted. However, the suggested procedure is extended to the intermittent flow in minichannels and it is also applied with success to horizontal macro tubes.

1. Introduction

Following Kandlikar and Grande (2003), minichannels are single tubes or multi-port extruded aluminum channels with inner hydraulic diameter in the range 0.2–3 mm. Understanding the forced convective condensation heat transfer mechanisms inside these channels is still somehow vague in comparison to the gained knowledge associated with conventional pipes. The lack of reliable heat transfer and pressure drop experimental data inside minichannels is due to rather difficult task in obtaining precise measurements on this scale and besides, there has been more interest dedicated to the flow boiling process associated with the intense heat removal. However, forced convective condensation is affected by gravity, viscous shear and surface tension. These forces influence flow regimes, pressure drops and heat transfer. Pressure drop during liquid-vapor flow within minichannels is affected by flow regime, while heat transfer is governed by frictional pressure drop as well.

There are three main issues involving pressure drop to be considered in the condensation heat transfer modeling. The first one refers to the saturation temperature drop due to the pressure drop along the channel, which namely increases the irreversibility of the heat transfer due to required higher driving temperature difference. The second issue instead, refers to higher energy consumption on the vapor–liquid interface. When the shear stress prevails over the surface tension and the gravity forces the liquid film gets thinner due to the liquid entrainment in the gas core. The thinner the liquid film the lower overall thermal resistance and thus a higher heat transfer coefficient is expected. However, higher energy consumption refers also to the third issue of the pressure drop consideration in the condensation heat transfer modeling. Higher shear stress leads to higher velocity gradient and thus higher temperature gradient in the thermal boundary layer. In this context Kosky and Staub (1971) associated heat transfer coefficient calculation with the frictional pressure gradient through the interfacial shear stress. The phenomenon stands for the increase of temperature gradient near the wall, that is, the increase in heat transfer coefficient, at the expense of frictional pressure drop along the pipe. While the first issue, associated to the saturation temperature drop due to the pressure drop, penalizes overall heat transfer rate, the other two issues enhance the condensation heat transfer coefficients. Indeed, one leads to the liquid layer decrease in thickness, whereas the other one stands for higher velocity gradient in the boundary layer.

It is though crucial to have reliable pressure drop prediction methods, for two-phase heat transfer or fluid flow modeling and

* Corresponding author.
E-mail address: luisa.rossetto@unipd.it (L. Rossetto).

0142-727X/$ - see front matter © 2008 Elsevier Inc. All rights reserved.
doi:10.1016/j.ijheatfluidflow.2008.09.003

Nomenclature

D	tube inside diameter, [m]
e_p	(percentage deviation) = 100 $(y_{CALC} - y_{EXP})/y_{EXP}$
e_R	(average deviation) = $(1/N_p)\Sigma e_p$
E	entrainment ratio
f	friction factor
g	gravitational acceleration, [m s^{-2}]
G	total mass velocity, [kg m^{-2} s^{-1}]
j_G	superficial gas velocity, [m s^{-1}]
J_G	dimensionless gas velocity=$x\ G/[g\ D_h\rho_G(\rho_L - \rho_G)]^{0.5}$
N_p	number of data points
p	pressure [Pa]
p_R	reduced pressure = p/p_c
Ra	arithmetical mean deviation of the assessed profile (according to ISO 4287 : 1997), [μm]
Re	Reynolds number
Re_L	$=G(1 - x)D_h/\mu_L$
Re_{LO}	$=G\ D_h/\mu_L$
Rr	relative roughness of the tube
Rz	maximum height of profile (according to ISO 4287: 1997), [μm]
T,t	temperature [K], [°C]
u_τ	friction velocity = $(\tau/\rho_L)^{0.5}$
x	vapour mass quality
z	axial coordinate oriented with the flow [m]
δ	liquid film thickness [m]
Δp	pressure difference [Pa]
ε	volume fraction of liquid in the film at the wall
Φ^2_{LO}	$(dp/dz)_f\ /(dp/dz)_{f,LO}$
μ	dynamic viscosity [kg m^{-1} s^{-1}]
ν	kinematic viscosity [m^2 s^{-1}]
ρ	density [kg m^{-3}]
σ	surface tension [N m^{-1}]
σ_N	(standard deviation) = $\{[\Sigma\ (e_p - e_R)^2]/(N_p - 1)\}^{1/2}$
τ	vapour shear stress on the liquid film [N m^{-2}]

Subscripts

an	annular
c	critical
CALC	calculated
EXP	experimental
f	frictional
G	gas phase; gas with its actual mass flow rate
GC	gas core
h	hydraulic
IN	at the inlet
L	liquid phase with its actual mass flow rate
LO	liquid phase with total mass flow rate
OUT	at the outlet
s	saturation
ss	stainless steel

optimization. As stated by Cavallini et al. (2006), no correlation was found to be able to predict satisfactory frictional pressure drop during liquid–vapor flow in different minichannels over wide range of test conditions. In this context, a generalized procedure development for calculation of the frictional pressure gradient during condensation or adiabatic liquid–vapor flow inside pipes with different hydraulic diameters and surface roughness is presented in this paper. Step-by-step development of the present correlation goes from precise selection and classification of the available experimental data through consideration of different effects to the comparison against selected models and some new experimental results. Both, modeling and experimental evaluation are presented herein over entire span of governing flow patterns. However, no flow visualization tests have been performed in this paper; instead, observations from different authors have been adopted for characterization of the flow regimes.

2. Available pressure drop models and observed flow patterns

2.1. Pressure drop models

Before developing a new model, present authors compared predictions from several models published in the open literature against the experimental data by Cavallini et al. (2005a). The models were either developed for conventional macrochannels, such as the ones by Friedel (1979, 1980) and Müller-Steinhagen and Heck (1986), or they were specifically developed for minichannels as those by Mishima and Hibiki (1996), Yan and Lin (1999), Chen et al. (2001), Zhang and Webb (2001), Garimella et al. (2004), Koyama et al. (2003). No model was able to predict with a satisfactory agreement frictional pressure drop for flow in minichannels of both high and low pressure fluids. Particularly, no model seems to be able to predict frictional pressure drops of R410A, while many models are not able to catch R236ea trends as well. Many correlations, on the contrary, were able to predict frictional pressure drops of R134a.

2.2. Flow patterns

Some researchers observed flow patterns during condensation of R134a in different minichannels. Even though no general flow regime map is available, all observations lead to the annular flow regime extension at the expense of wavy flow suppression as hydraulic diameter is decreased.

Coleman and Garimella (1999, 2000a,b) reported flow patterns during condensation of R134a inside horizontal tubes and square minichannels. The hydraulic diameters were ranging from 1 to 4.9 mm, while mass velocities have always been set above 150 kg m^{-2} s^{-1}. The authors observed annular, wavy, intermittent (slug, plug) and dispersed (bubble) flow patterns. At smaller hydraulic diameters (<1 mm) the wavy regime was not present while at high flow rates and qualities annular film and mist or mist flows prevailed. With R134a at 52 °C in square minichannels of diameter 1 or 2 mm mist flow was present for dimensionless gas velocity (J_G) higher than 10–15. The authors found tube shape to be less significant, while hydraulic diameter had a substantial effect on flow transitions. Wang et al. (2002) also reported flow patterns for condensation of R134a at 35 °C saturation temperature. They used multi-port rectangular minichannels with D_h = 1.46 mm and mass velocities ranging from 75 to 350 kg m^{-2} s^{-1}. The authors observed annular, wavy and slug flow, while the flow was always annular for $J_G > 2.5$. Also Kim et al. (2003) observed annular, slug and bubbly flow during condensation of R134a in a horizontal circular single minichannel of diameter 0.75 mm. They performed experiments at 40 °C saturation temperature and mass velocities ranging between 100 and 600 kg m^{-2} s^{-1}.

3. Modelling

3.1. Correlation for annular and mist flow ($J_G > 2.5$) in smooth minichannels

In order to test equations for frictional pressure gradient during flow of refrigerants in minichannels, the present authors have

collected a wide data bank of experimental values from different authors. Out of this data bank only data for flow in smooth minichannels with dimensionless gas velocity greater than 2.5 have been selected in order to be sure to have data points in annular and mist flow. In Table 1 authors reference, type of channels, hydraulic diameter, fluid, saturation temperature, mass velocity and number of data points used are reported. The Coleman (2000) pressure drop data has been taken during adiabatic and condensing flow of R134a at $p_R = 0.37$ in channels with circular and square cross section with $0.51 \leqslant D_h \leqslant 1.52$ mm. Coleman estimated the relative roughness being from 10^{-4} to 5×10^{-4} for the circular channels and 9×10^{-4} for the square ones. The Zhang (1998) and Hirofumi and Webb (1995) (reported in Zhang (1998)) pressure drop data refer to adiabatic flow of R134a in circular and square cross section multiport channels and in a single minitube with plain inner surface. Reduced pressure for R134a was varied between 0.25 and 0.47. The Jeong et al. (2005) data has been measured during adiabatic flow of R744 in square cross section channels. Cavallini et al. (2006) presented a review of available data.

The data bank contains the Cavallini et al. (2004, 2005a) data for three different fluids. The R134a data by Cavallini et al. (2004, 2005a) have been plotted in the Coleman and Garimella map for channels with a square cross section, for hydraulic diameters equal 1 and 2 mm: all the R134a data were in the annular, annular-mist, mist flow regimes. Recent data are mostly associated to R134a, while only few experiments have been reported at significantly different reduced pressure conditions. In this matter, Cavallini et al. (2004, 2005a) extended the available experimental data with experiments during adiabatic flow of R134a, R236ea and R410A inside 1.13 m long multi-port minichannel test section. The experiments have been performed at 40 °C saturation temperature and mass velocities ranging from 200 to 1400 kg m^{-2} s^{-1} within square channels with hydraulic diameter 1.4 mm. The arithmetic mean deviation of the assessed profile (Ra) of the inner surface was 0.08 μm while the maximum height of profile (Rz) was 0.43 μm. The three refrigerants were chosen because they present a wide range of reduced pressures at given test conditions. In fact at 40°C saturation temperature the reduced pressure of R236ea is around 0.1, 0.25 for R134a and 0.5 for R410A. The pressure drop is obtained by measuring the saturation temperature drop in the tube, by means of one T-type thermopile and two T-type thermocouples fixed to the aluminium tube. Experimental uncertainty of the non intrusive measuring technique was deduced from the experimental error of the thermopile used in the measurement. The ±0.03 K leads to an experimental nominal uncertainty of ±0.71 kPa m^{-1} for R134a, ±1.6 kPa m^{-1} for R410A and ± 0.28 kPa m^{-1} for R236ea at the same average saturation temperature (40 °C).

The following equation, which interpolates the multiport data of Table 1, Cavallini et al. (2004, 2005a), Coleman (2000), Zhang (1998), Hirofumi and Webb (1995), with an absolute deviation of 11.3%, was obtained by Cavallini et al. (2005b):

$$\left(\frac{dp}{dz}\right)_f = \Phi_{LO}^2 \left(\frac{dp}{dz}\right)_{f,LO} = \Phi_{LO}^2 2 f_{LO}^* \frac{G^2}{D_h \rho_L} \tag{1}$$

$$f_{LO}^* = 0.046 Re_{LO}^{-0.2} = 0.046 \left(\frac{G D_h}{\mu_L}\right)^{-0.2} \text{ for any } \mathbf{Re}_{LO} \tag{2}$$

*The friction factor from Eq. (2) refers to surfaces with negligible surface roughness.

$$\Phi_{LO}^2 = Z + 3.595 \cdot F \cdot H \cdot (1-E)^W \tag{3}$$

$$W = 1.398 p_R \tag{4}$$

$$Z = (1-x)^2 + x^2 \frac{\rho_L}{\rho_G} \left(\frac{\mu_G}{\mu_L}\right)^{0.2} \tag{5}$$

$$F = x^{0.9525} (1-x)^{0.414} \tag{6}$$

$$H = \left(\frac{\rho_L}{\rho_G}\right)^{1.132} \left(\frac{\mu_G}{\mu_L}\right)^{0.44} \left(1 - \frac{\mu_G}{\mu_L}\right)^{3.542} \tag{7}$$

3.2. Liquid entrainment

The above Eqs. (1)–(9) give the two phase multiplier as a function of vapor quality, of liquid and vapor properties, of reduced pressure and of the entrained liquid fraction E. The liquid entrainment appears during shear dominated flow regime, where the shear stress is responsible for the separation of the liquid drops from the liquid-vapor interface. Since the entrained liquid in the gas core virtually increases density of the vapor phase, its effect is similar to the increase in reduced pressure. Besides, as the liquid film gets thinner the liquid interface roughness decreases (Hewitt and Hall-Taylor (1970)); hence, in a tube with a given gas flow rate, the pressure gradient is decreased. Indeed, entrainment acts to reduce the two phase multiplier, which may also be true for flow in minichannels. The entrainment ratio in Eq. (3) has to be calculated as suggested by Paleev and Filippovich (1966):

$$E = 0.015 + 0.44 \cdot \log\left[\left(\frac{\rho_{GC}}{\rho_L}\right)\left(\frac{\mu_L j_G}{\sigma}\right)^2 10^4\right] \tag{8}$$

if $E \geqslant 0.95$ $\quad E = 0.95$
if $E \leqslant 0$ $\quad E = 0$

The homogeneous gas core density ρ_{GC}:

$$\rho_{GC} = \left(\frac{x + (1-x)E}{\frac{x}{\rho_G} + \frac{(1-x)E}{\rho_L}}\right)$$
$$\rho_{GC} \approx \rho_G \left(1 + \frac{(1-x)E}{x}\right) \text{ for } \rho_L \gg \rho_G \tag{9}$$

The above correlation was developed for macro-tubes, it neglects the diameter effect, the surface roughness and the liquid Reynolds number dependence. As stated by the authors and by Ishii and Mishima (1989), the calculated values are in good agreement with a limited number of air-water data points for vertical macro-tubes. Furthermore, the present authors observed also a

Table 1
Frictional two-phase pressure drop experimental studies inside plain horizontal minichannels J_G> 2.5 (annular and mist flow)

Author	Channel[a]	D_h [mm]	Fluid	t_s [°C]	G[kg m^{-2} s^{-1}]	N_p	Experimental uncertainties		
							P [kPa]	ΔP [Pa]	x
Cavallini et al. (2004, 2005a)	M–S	1.4	R134a, R236ea, R410A	40	200–1400	66	±5	±392–2240	±4%
Coleman (2000)	M–C, M–S	1.52, 0.76, 0.51, 0.76	R134a	55	150–750	171		±15.6–620	±3–8%
Hirofumi and Webb (1995)	M–C, M–S	2.13, 1.45, 0.96, 1.33	R134a	65	200–620	18	±8.3	±77.5–465	±1.78–8.7%
Zhang (1998),	M–C	2.13	R134a	40, 65	200–600	17	±8.3	±77.5–465	±1.78–8.7%
Zhang and Webb (2001)	Si–C	3.25	R134a, R22,R404a	25–50	400–1000	54	±8.3	±77.5–465	±1.78–8.7%
Jeong et al. (2005)	M–S	2.0	R744	0,5,10	700	21	–	–	–

[a] M: multi-port; Si: single channel; R: rectangular; C: circular; S: square.

good agreement between predictions from Eqs. (8) and (9) and the R113 experimental data by Lopez de Bertodano et al. (2001). The experiments associated to a low viscosity and a low surface tension fluid as compared to water have been performed in a vertical tube with inner diameter 9.53 mm. Pan and Hanratty (2002) stated that in horizontal macro tubes only for very large dimensionless gas velocities J_G (between 6 and 12 for their air water experimental data) entrainment could be described by equations for vertical tubes, while for small gas velocities gravitational settling of the drops should be taken into account. Since the Paleev and Filippovich (1966) equation is here applied to horizontal minichannels, the gravitational effects are certainly low. Therefore, the gravitational settling of the drops is not considered in the present study.

A comparison between predictions from Eqs. (1)–(9) and experimental data presented in the Table 1 is given in Fig. 1, where the lines +20% and −30% refer to deviations from "perfect" agreement. Standard and relative deviations between predictions from the above model and experimental data are reported in Table 2. Moreover, the present correlation has been found to predict Cavallini et al. (2005a) data, particularly for high pressure fluid R410A, better than the models cited in Section 2.1. The calculated frictional pressure gradient profiles for flows of R134a, R410A and R236ea in a 1.4 mm hydraulic diameter minichannel have been plotted in Fig. 2 along with experimental values by Cavallini et al. (2004, 2005a).

Properties of the refrigerants have been calculated with Refprop 7.0 by NIST (2002).

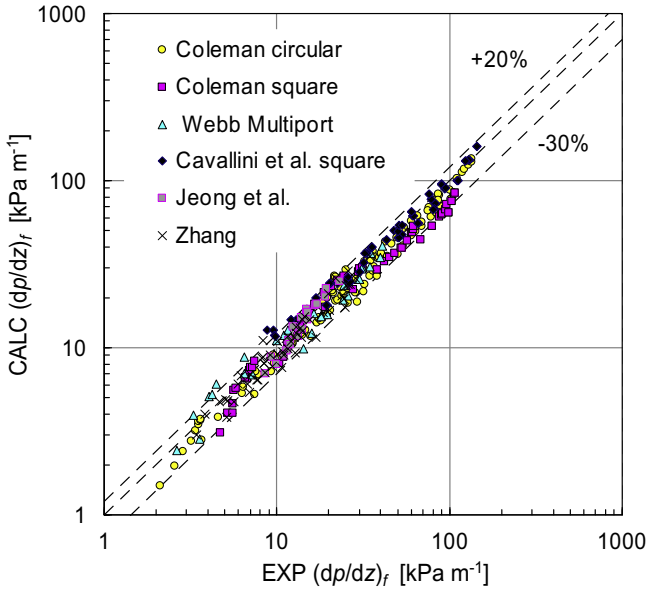

Fig. 1. Comparison between predictions from Eqs. (1)–(9) and experimental data of Table 1.

Table 2
Standard deviations and relative deviations for present model compared with experimental data of Table 1

Author	N_p	σ_N [%]	e_R [%]
Cavallini et al. (2004, 2005a)	66	12.6	3.4
Coleman (2000)	171	12.5	−12.6
Zhang (1998), Hirofumi and Webb (1995): multiport	35	16.7	−1.3
Zhang (1998), Zhang and Webb (2001) single tube	54	14.7	−9.4
Jeong et al. (2005)	21	12.4	−3.0

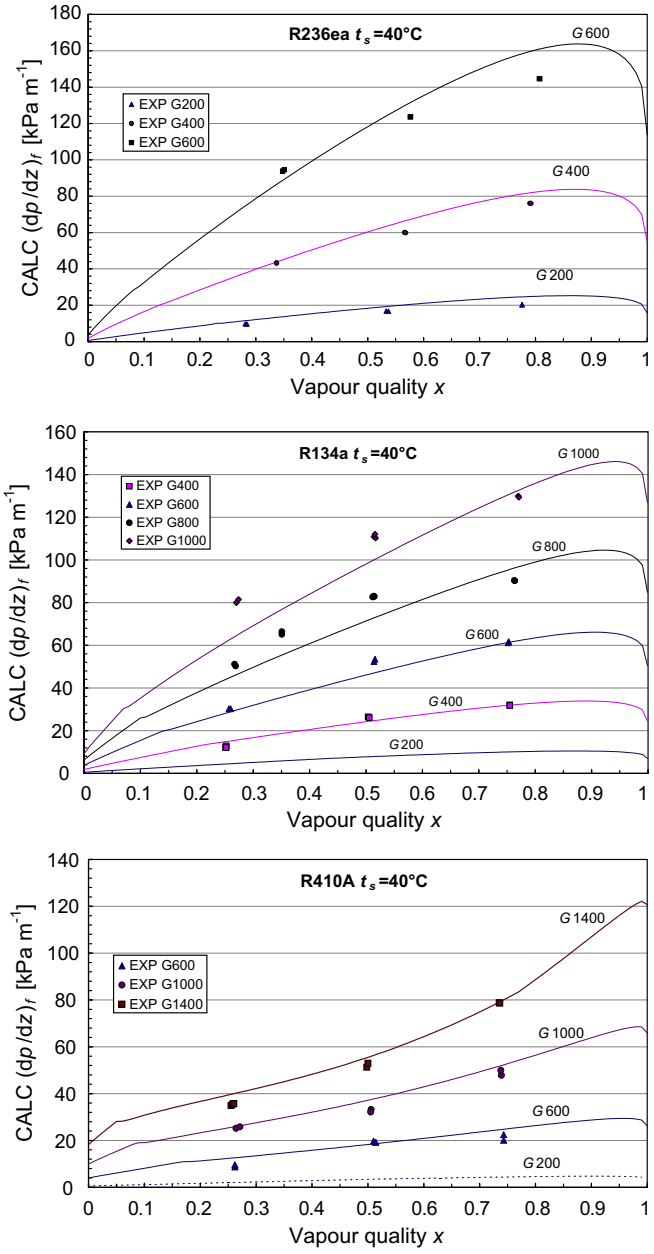

Fig. 2. Comparison between predictions from Eqs. (1)–(12) and experimental data by Cavallini et al. (2005a).

3.3. Microfinned minichannels

Further comparisons are given in Fig. 3, where it is shown that predictions from Eqs. (1)–(9) are in good agreement with 58 experimental frictional pressure gradients at $J_G > 2.5$ by Webb and Ermis (2001) ($e_R = 9.3\%$, $\sigma_N = 20.9\%$). These frictional pressure gradients refer to R134a adiabatic data at 65°C saturation temperature and mass velocities in the range from 300 to 1000 kg m^{-2} s^{-1}. The authors have used multiport aluminium tubes with inner microfins and hydraulic diameters 0.611 mm, 1.56 mm and 0.44 mm. Fin heights range from 0.13 mm to 0.25 mm. Reported experimental uncertainties are similar to those by Zhang (1998).

3.4. Extension of the model to $J_G < 2.5$

The present frictional pressure gradient model was also extended to lower vapour qualities and mass velocities. When

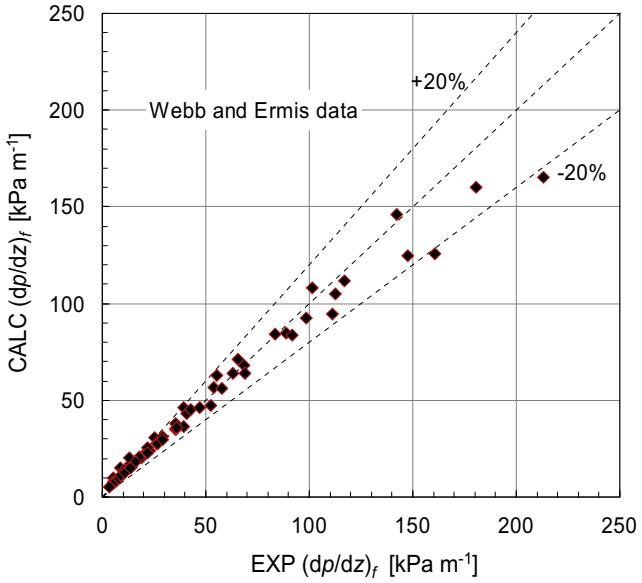

Fig. 3. Comparison between predictions from Eqs. (1)–(9) and experimental data by Webb and Ermis (2001) for microfinned minichannels.

$J_G < 2.5$ the higher value between $(dp/dz)_f$ from Eqs. (1)–(9) and the all liquid frictional pressure gradient $(dp/dz)_{f,LO}$ from Eqs. (10)–(12) is selected

$$\left(\frac{dp}{dz}\right)_{f,LO} = 2f_{LO}\frac{G^2}{D_h\rho_L} \tag{10}$$

$$\text{for } Re_{LO} > 2000 \quad f_{LO} = 0.046[GD_h/\mu_L]^{-0.2} \tag{11}$$

$$\text{for } Re_{LO} < 2000 \quad f_{LO} = C/[GD_h/\mu_L]$$
$$C = 16 \text{ circular section}, \quad C = 14.3 \text{ square section} \tag{12}$$

Available data at $J_G < 2.5$ by Cavallini et al. (2001), Coleman (2000) and Zhang (1998) is compared versus predictions from the model above, (Eqs. (1)–(12)). Even though the data by Coleman (2000) is generally underestimated, the overall agreement is satisfactory (Fig. 4).

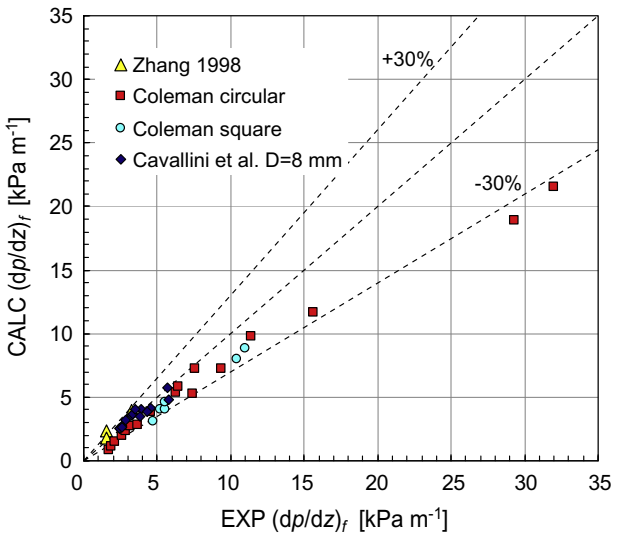

Fig. 4. Comparison between predictions from Eqs. (1)–(12) and available experimental data with $J_G < 2.5$.

3.5. Macro tubes

Cavallini et al. (2001) measured pressure drops during condensation of several HFC refrigerants (R134a, R125, R32, R410A and R236ea) inside a horizontal macro tube of inner diameter 8 mm. Dimensionless gas velocities were always less than 10, while mass velocities were ranging from 100 to 750 kg m^{-2} s^{-1}. Experimental uncertainty of differential pressure was ±60 Pa. Predictions from Eqs. (1)–(12) are in good agreement with experimental frictional pressure gradients by Cavallini et al. (2001), if no entrainment effects are taken into account in the calculation, which means $E = 0$ in Eq. (3). Comparisons are shown in Fig. 5, for 158 data points with $2.5 < J_G < 10$ ($e_R = -7.0\%$, $\sigma_N = 9.0\%$).

3.6. Calculated trends of the model

Figs. 6 and 7 show the frictional pressure gradient trends versus vapour quality associated to R410A adiabatic flow in 1.4 mm and

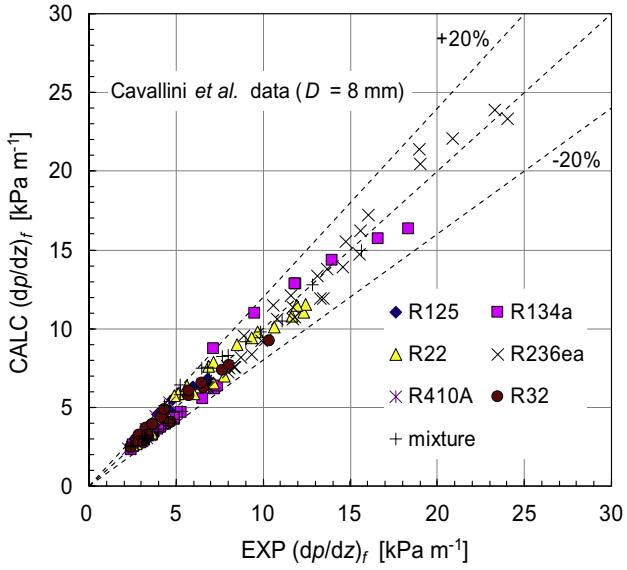

Fig. 5. Comparison between predictions from Eqs. (1)–(9) and experimental data by Cavallini et al. (2001) for circular macro tube with inner diameter equal 8 mm.

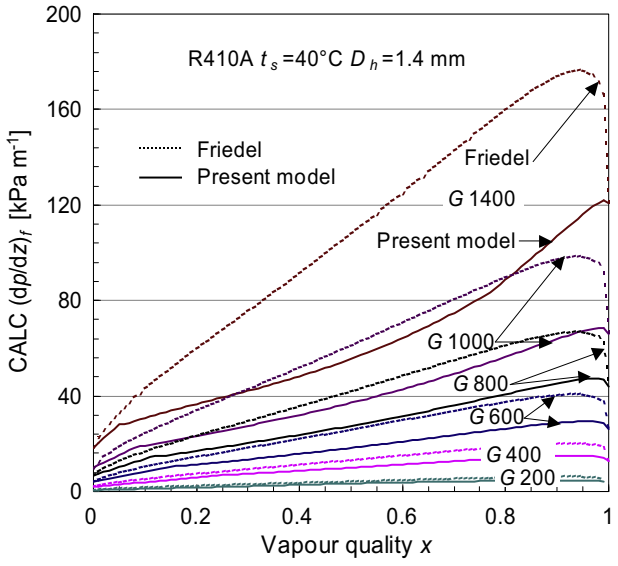

Fig. 6. Comparison between predictions from present model Eqs. (1)–(12) and the Friedel (1979, 1980) model, both applied for R410A in minichannel.

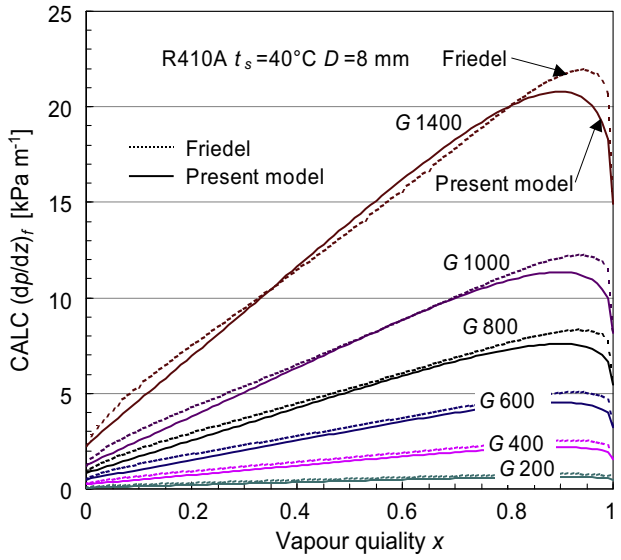

Fig. 7. Comparison between predictions from present model Eqs. (1)–(12) and the Friedel (1979, 1980) model, both applied for R410A in macro tube.

8 mm inner diameter tubes. The frictional pressure gradient trends are calculated by the present model and the model by Friedel (1979, 1980). Predicted values from the two models agree for the macro tube while they are very different for the minichannel. The Friedel equation overestimates the pressure gradient of the high pressure refrigerant R410A, when flowing in minichannels with negligible surface roughness (Cavallini et al., 2006).

4. Extension of the model for the not-negligible surface roughness

The multiport minichannel tested by Cavallini et al. (2004, 2005a) is characterized by a square cross section and a low value of surface roughness (Ra = 0.08 and Rz = 0.43 μm), where effect can thus be neglected. However, surface roughness affects pressure drop during single phase flow in macrochannels and minichannels, as shown by Taylor et al. (2006). To investigate the effect of tube wall roughness and channel geometry on the two-phase frictional pressure gradient, the present authors report here the pressure drop measured during condensation and adiabatic flow of R134a in a single circular mini-tube with much higher surface roughness as compared to the previously tested minichannel.

The test rig and experimental procedures used for measuring the pressure drop in the round minichannel are fully described in Cavallini et al. (2007) and Matkovic (2006). The test tube is a commercial copper tube with inner diameter 0.96 mm and 228.5 mm length. The arithmetical mean deviation of the assessed profile of the inner surface is 1.3 μm while the maximum height of profile is 10 μm. These values are much higher than those of the multiport extruded aluminium channel. The inlet and outlet pressure ports are inserted in two stainless steel tubes 24 mm apart from the copper tube. The stainless tubes have 0.762 mm inner diameter, Ra = 2.0 μm and Rz = 10.2 μm. The total frictional pressure drop is then the sum of the frictional pressure drop in the two stainless steel tubes, each 24 mm long, of the frictional pressure drop in the copper tube 228.5 mm long and of the pressure variations due to abrupt enlargement (from 0.762 mm diameter to 0.96 mm diameter) and contraction (from 0.96 mm to 0.762 mm). The experimental uncertainty for the measured pressure difference is ±0.1 kPa, for absolute pressure is ±3 kPa, for refrigerant flow rate is ±0.2% and for vapour quality ±1%.

First of all single-phase pressure drop experiments were performed to gain critical insight into the test section hydraulic performance. The frictional pressure drop in the copper tube is obtained from the total measured pressure drop by subtracting the local losses and the pressure loss in the stainless steel sectors

$$\Delta p_{\text{Cu·tube}} = \Delta p_{\text{total}} - \sum \Delta p_{\text{local}} - \Delta p_{\text{ss·tube}} \tag{13}$$

The abrupt enlargement and contraction pressure variations were estimated according to Idelchik (1996). These calculated local values, that were less than 6% of the total measured value, were subtracted from the total experimental pressure drop.

The pressure variation in the stainless steel tube is calculated with the equation:

$$\Delta p_{\text{ss·tube}} = 2 f_{\text{ss}} \frac{L_{\text{ss}} G_{\text{ss}}^2}{D_{\text{ss}} \rho} \tag{14}$$

where the friction factor f_{ss} is estimated with the proper equation according to the corresponding Reynolds number, as reported in the Appendix (Eqs. (A1)–(A4)).

Fig. 8 shows the calculated friction factor for the copper tube against the Reynolds number in the same tube, being the friction factor defined as

$$f_{\text{Cu·tube}} = \Delta p_{\text{Cu·tube}} \frac{D_{\text{Cu·tube}} \rho}{2 L_{\text{Cu·tube}} G_{\text{Cu·tube}}^2} \tag{15}$$

The new experimental single phase friction factors are successfully compared against predictions by Hagen–Poiseuille, Blasius and Teplov as well as by Churchill (1977) model over the entire range of Reynolds numbers (Fig. 8). For transition and turbulent region the relative roughness of the channel was assumed to be equal to 2 · Ra/D. All the single phase pressure drop experiments reported here refer to adiabatic flows. Low Reynolds number data is measured during subcooled liquid tests, whereas data at high Reynolds numbers was measured with superheated vapour. Nevertheless, diabatic single-phase pressure loss measurements were also performed in a wide range of test conditions both during heating and cooling mode. No significant difference in the frictional pressure gradient measurements was found by comparing the diabatic experimental results to the adiabatic data.

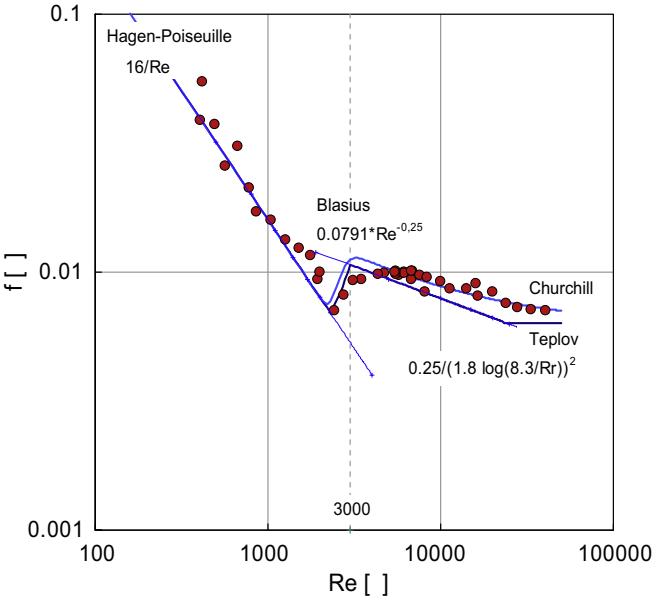

Fig. 8. Experimental and calculated friction factor for a 0.96 mm inner diameter circular single minichannel.

Adiabatic two-phase pressure drop tests were also performed during R134a flow in the same test section as described above. Fig. 9a shows the total experimental pressure drop for R134a at 40 °C versus vapour mass quality, at three mass flow velocities (referred to the copper tube flow cross sectional area): 400, 600 and 800 kg m^{-2} s^{-1}. The total pressure drop is the sum of pressure variations in the stainless steel tubes, in the copper tube and in the two abrupt geometry changes

$$\Delta p_{\text{total}} = \sum \Delta p_{\text{local}} + \Delta p_{\text{Cu·tube}} + \Delta p_{\text{ss·tube}} \tag{16}$$

Fig. 9a and b show the comparison between the experimental Δp_{total} data and the calculated values with the above model (Eqs. (1)–(12)) for linear losses and according to Paliwoda (1992) for abrupt geometry changes. Pressure variations for geometry changes were around 10% of the overall calculated value. The model underestimates experimental pressure drop by 20%. First of all one must consider that the present test section is made of a single round channel, whereas most of the data used in Figs. 1 and 2 refer to multiport tubes, with square cross sections in some cases.

Besides, in comparison with the aluminium extruded tube tested by the present authors, the copper mini tube presents a considerably higher surface roughness. Therefore, a possible explanation of the discrepancy in Fig. 9 can be related to the surface roughness of the tube. In order to enlight the effect of the roughness in the minichannel, one can calculate the liquid film thickness δ at the wall by using the model by Cavallini et al. (2006), based on Kosky and Staub (1971) model

$$\delta = \frac{\delta^+ \cdot \nu_L}{u_\tau} = \frac{\delta^+ \cdot \nu_L}{\tau^{0.5}} \rho_L^{0.5} = \frac{\delta^+ \cdot \nu_L}{\left[\left(\frac{dp}{dz}\right)_f \frac{D}{4}\right]^{0.5}} \rho_L^{0.5} \tag{17}$$

with

$$\delta^+ = \left(\frac{Re_L}{2}\right)^{0.5} \qquad Re_L < 1145$$

$$\delta^+ = 0.0504 Re_L^{7/8} \qquad Re_L > 1145$$

$$Re_L = \frac{GD(1-x)(1-E)}{\mu_L}$$

and the frictional pressure gradient from Eqs. (1)–(12).

Since most of the experimental data refer to high vapour qualities ($x > 0.7$), the dimensionless film thickness calculated with the equations above, assuming no entrainment is occurring, is less than 30, which means that the liquid film is laminar near the wall and in the transition to turbulent flow far from the wall. It corresponds to a liquid film $\delta < 25$ μm, when $E = 0$ and $x = 0.75$. With entrainment calculated from Eqs. (8) and (9), the thickness of the liquid film at the wall is around 10–15 μm ($x = 0.75$, $400 \leqslant G \leqslant 800$ kg m^{-2} s^{-1}). Therefore, the surface roughness, with peaks up to 15 μm high, certainly affects the laminar and the laminar-turbulent transition sublayers. The liquid flow is influenced by both the vapour shear stress and the surface roughness. At high mass velocities ($G \geqslant 400$ kg m^{-2} s^{-1}) the liquid laminar sublayer ($\delta^+ < 5$) has a thickness $\delta < 8$–10 μm. When the height of the peaks is bigger than the liquid film thickness, the liquid film may also be influenced by the surface tension in the valleys between the peaks. All these effects are not present in the aluminium extruded tubes because of the lower surface roughness.

In the end, it can be concluded that the surface roughness affects the motion of the liquid film. There is no evidence though that also the liquid entrainment is affected by the surface roughness, except for the case when the peaks in the surface are in the same height range as the liquid film thickness. With regard to the data presented above, it should also be considered that the geometry of the channel may play a role on the liquid entrainment: the presence of corners, in fact, should be in favour of a higher entrainment due to the combined effect of surface tension and shear stress. Unfortunately, the data available does not allow to clearly detect the effect of the geometry in minichannels and, with regard to data by the present authors, to single out the effect of roughness from the one due to the geometry.

4.1. Extension of the model to include the effect of surface roughness

The above discussion points out the necessity to take into account surface roughness when calculating the frictional pressure gradient for two-phase flow in mini and microchannels. Recently Agarwal and Garimella (2006) also correlated the two-phase frictional pressure drops in minichannels with surface roughness. Beside this they suggested different coefficients for their different channel shapes.

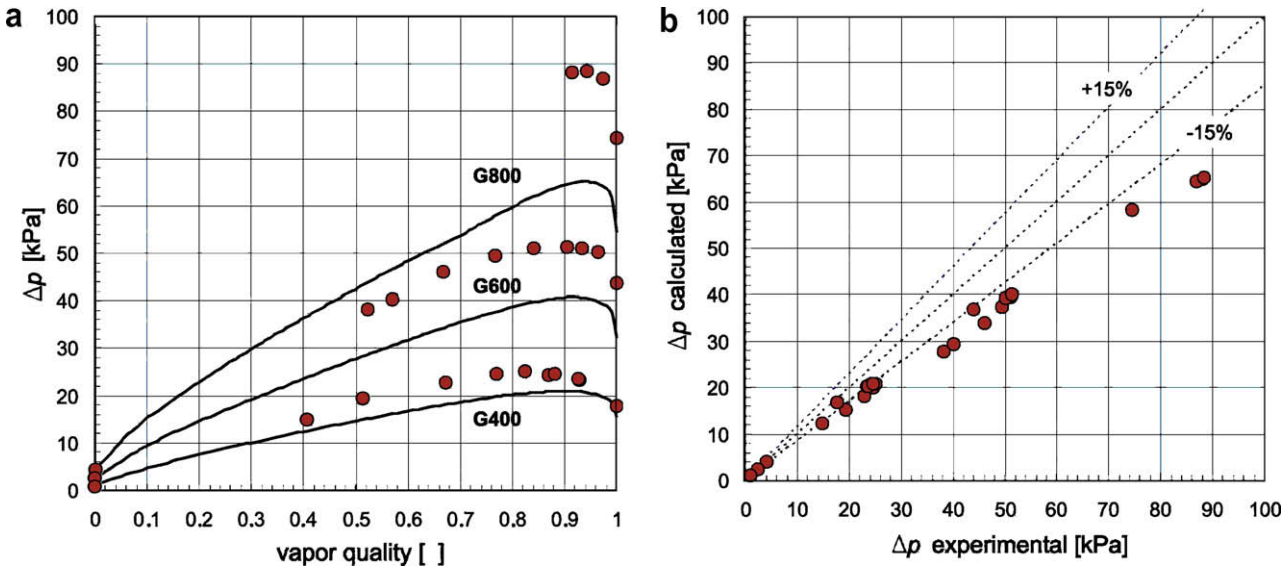

Fig. 9. (a) Overall experimental pressure losses and calculated trends, by the model for smooth tubes (Eqs. (1)–(12)), during adiabatic two-phase flow of R134a at three different mass velocities. (b) Calculated vs experimental pressure drop.

In order to consider the effect of the tube wall roughness, the liquid friction factor of the above model (Eq. (2)) is corrected in the following way

$$f^*_{LO} = 0.046 Re_{LO}^{-0.2} + 0.7\frac{2Ra}{D_h} \quad \text{for} \quad \frac{2Ra}{D_h} < 0.0027 \tag{18}$$

The above friction factor is in good agreement with the Churchill curve in the range $3000 < Re_{LO} < 6000$. In Fig. 10 experimental values of the cumulative adiabatic two-phase pressure drops are compared with predicted values from the model modified with Eq. (18). Agreement is satisfactory, even if data is a little underestimated at high mass velocities and vapour qualities, suggesting channel shape effects or weakening of entrainment due to wall roughness.

Finally, pressure drop measurements have also been performed during condensation of R134a in the copper minitube with inner diameter 0.96 mm. Experiments have been performed at three mass velocities: 400, 600 and 800 kg m^{-2} s^{-1} and with vapour qualities varying from 0.95 to 0.12. The total measured pressure variation is the sum of Δp_{total} from Eq. (16) and the pressure gain due to momentum change Δp_m. This last term can be estimated as in the following. Assuming that the gas core and the entrained liquid flow with the same velocity, as suggested by Hewitt and Hall-Taylor (1970), the vapour–liquid mixture in the core has density ρ_{GC} (Eq. (9)) and velocity u_{GC} from

$$u_{GC} = \frac{G[x + (1-x)E]}{(1-\varepsilon)\rho_{GC}} \tag{19}$$

where ε is the volume fraction of the liquid film as function of the liquid film thickness from Eq. (17):

$$\varepsilon = 1 - \left(\frac{D - 2\delta}{D}\right)^2 \tag{20}$$

The differential pressure gain due to momentum change is the sum of the term due to the liquid in the film at the wall and the quantity due to the liquid–vapour mixture in the core:

$$(-\mathrm{d}p)_m = G^2 \mathrm{d}\left[\frac{(1-x)^2(1-E)^2}{(\varepsilon)\rho_L} + \frac{[x + (1-x)E]^2}{(1-\varepsilon)\cdot\rho_{GC}}\right] \tag{21}$$

The pressure variation due to momentum change becomes

$$(-\Delta p)_m = G^2\left[\frac{(1-x_{IN})^2(1-E_{IN})^2}{(\varepsilon_{IN})\rho_L} + \frac{[x_{IN} + (1-x_{IN})E_{IN}]^2}{(1-\varepsilon_{IN})\cdot\rho_{GC,IN}}\right] - G^2\left[\frac{(1-x_{OUT})^2(1-E_{OUT})^2}{(\varepsilon_{OUT})\rho_L} + \frac{[x_{OUT} + (1-x_{OUT})E_{OUT}]^2}{(1-\varepsilon_{OUT})\cdot\rho_{GC,OUT}}\right] \tag{22}$$

The comparison between the measured experimental values and predictions from the modified model gives percentage deviations e_p in the range 5–28%.

5. Conclusions

A model to compute the frictional pressure gradient during condensation and adiabatic flow in minichannels is presented. The correlation is validated against data measured in minichannels with hydraulic diameters ranging from 0.5 mm to 3.2 mm. Adiabatic flow or condensing flow of halogenated refrigerants with reduced pressure between 0.1 and 0.6 was always set above 150 kg m^{-2} s^{-1} mass velocity. Since the present correlation has been devoted to pressure drop prediction during shear dominated flow regimes, only data with $J_G > 2.5$ from different authors has been used in the modelling. Nevertheless, values associated to intermittent flow can also be predicted by simple selection between the present correlation and the all liquid frictional pressure gradient. On the other hand, at high vapour velocities, the present correlation takes into account also the effect of the liquid entrainment rate in the gas core. The model adopts a simplified equation for the entrainment rate, which depends on gas velocity, vapour quality and thermodynamic properties. However, further improvement may be to investigate the dependence of the entrainment rate in minichannels on the channel geometry and channel size.

Furthermore, surface roughness effects on the liquid–vapor flow are discussed in the article. New experimental frictional pressure gradient data considering single-phase flow and adiabatic two-phase flow of R134a inside a single horizontal mini tube, with 0.96 mm inner diameter and with not-negligible surface roughness, is presented in the paper. In order to account for the effect of surface quality, a simple modification of the liquid friction factor has been introduced in the model. The new single phase data is

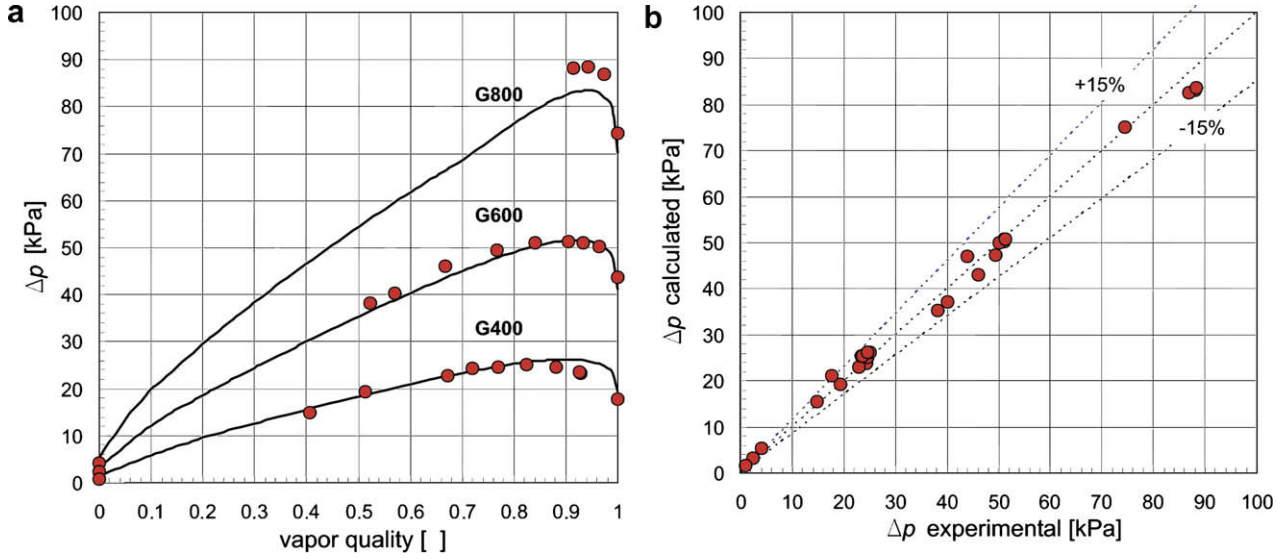

Fig. 10. (a) Overall experimental pressure losses and calculated trends by the present model (modified with Eq. (18)) during adiabatic two-phase flow of R134a at three different mass velocities. (b) Calculated vs experimental pressure drop.

successfully compared against predictions by Hagen–Poiseuille, Blasius and Teplov as well as by Churchill (1977) model over entire range of Reynolds numbers assuming a relative roughness of the channel equal to 2 · Ra/D.

Finally, overall predictions from the model are in good agreement with experimental data attributed to channels or tubes with different surface roughness, different hydraulic diameters and different fluids. The suggested procedure is successfully extended to the intermittent flow in minichannels and it is also applied with success to horizontal macro tubes.

Acknowledgement

The support of the EC through the Project HPRN-CT-2002-2004 and of the MIUR through the PRIN program is gratefully acknowledged.

Appendix

In details, the friction factor f in single phase flow in the stainless steel tube is estimated in laminar flow, for $Re < 2300$, as

$$f_{\text{laminar}} = \frac{16}{Re_{\text{ss}}} = \left(\frac{16\mu}{D_{\text{ss}} G_{\text{ss}}}\right) \tag{A1}$$

and in turbulent flow, for $Re > 3\,000$, using the Blausius equation:

$$f_{\text{Blausius}} = 0.079 Re_{\text{ss}}^{-0.25} = 0.079\left(\frac{\mu}{D_{\text{ss}} G_{\text{ss}}}\right)^{0.25} \tag{A2}$$

up to the intersection with the Teplov equation (Idelchik (1996)) for rough tubes

$$f_{\text{Teplov}} = 0.25\left(\frac{1}{1.8\log(8.3/Rr_{\text{ss}})}\right)^2 \tag{A3}$$

with $Rr = 2\ Ra/D$.

In the transition region, for $2300 \leqslant \text{Re} \leqslant 3000$

$$f_{\text{transition}} = \frac{f_{\text{Blausius},Re=3000} - f_{\text{laminar},Re=2300}}{3000-2300}(Re_{\text{ss}} - 2300) + f_{\text{laminar},Re=2300} \tag{A4}$$

References

Agarwal, A., Garimella, S., 2006. Modeling of pressure drop during condensation in circular and non-circular microchannels. In: Proceedings of the IMECE 2006, IMECE2006-14672, ASME, Chicago.

Cavallini, A., Censi, G., Del Col, D., Doretti, L., Longo, G.A., Rossetto, L., 2001. Experimental investigation on condensation heat transfer and pressure drop of new HFC refrigerants (R134a, R125, R32, R410A, R236ea) in a horizontal tube. International Journal of Refrigeration 24 (1), 73–87.

Cavallini, A., Del Col, D., Doretti, L., Matkovic, M., Rossetto, L., Zilio, C., 2004. Measurement of pressure gradient during two-phase flow inside multi-port mini-channels. In: Pisa, G.P., Celata, et al. (Eds.), Proceedings of the Third International Symposium on Two-Phase Flow Modelling and Experimentation, September 22–24.

Cavallini, A., Del Col, D., Doretti, L., Matkovic, M., Rossetto, L., Zilio, C., 2005a. Two-phase frictional pressure gradient of R236ea, R134a and R410A inside multi-port mini-channels. Experimental Thermal and Fluid Science 29 (7), 861–870.

Cavallini, A., Rossetto, L., Matkovic, M., Del Col, D., 2005b. A model for frictional pressure drop during vapour–liquid flow in minichannels. In: IIR International Conference Thermophysical Properties and Transfer Processes of Refrigerants, 31 August–2 September, Vicenza Italy, pp. 71–78.

Cavallini, A., Doretti, L., Matkovic, M., Rossetto, L., 2006. Update on condensation heat transfer and pressure drop in minichannels. Heat Transfer Engineering 27 (4), 74–87.

Cavallini, A., Del Col, D., Matkovic, M., Rossetto, L., 2007. Local heat transfer coefficient during condensation inside a single minichannel. In: Sixth International Conference on Enhanced, Compact and Ultra-Compact heat Exchangers: Science, Engineering and Technology, Postdam, Germany, September 16–21.

Chen, I.Y., Yang, K.-S., Chang, Y.-J., Wang, C-C., 2001. Two-phase pressure drop of air–water and R-410A in small horizontal tubes. International Journal of Multiphase Flow 27 (7), 1293–1299.

Churchill, S.W., 1977. Friction factor equation spans all fluid-flow regimes. Chemical Engineering 45, 91–92.

Coleman, J.W., 2000. Flow visualization and pressure drop for refrigerant phase change and air–water flow in small hydraulic diameter geometries. Ph.D. Thesis, Iowa State University, Ames Iowa.

Coleman, J.W., Garimella, S., 1999. Characterization of two-phase flow patterns in small diameter round and rectangular tubes. International Journal of Heat and Mass Transfer 42 (15), 2869–2881.

Coleman, J.W., Garimella, S., 2000a. Two-Phase flow regime transitions in microchannel tubes: the effect of hydraulic diameter. ASME HTD-366-4, 71-83.

Coleman, J.W., Garimella, S., 2000b. Visualization of refrigerant two-phase flow during condensation. In: Proceedings of the NHTC'00, NHTC2000-12115, ASME, New York.

Friedel, L., 1979. Improved friction pressure drop correlations for horizontal and vertical two-phase pipe flow. In: Proceedings of the European Two-phase Flow Group Meeting, Ispra, Paper E2.

Friedel, L., 1980. Pressure drop during gas/vapor–liquid flow in pipes. International Chemical Engineering 20 (3), 352–367.

Garimella, S, Agarwal, A., Killon, J.D., 2004. Condensation pressure drops in circular minichannels. In: Second International Conference on Microchannels and Minichannels, Rochester, pp. 649–656.

Hewitt, G.F., Hall-Taylor, N.S., 1970. Annular two-phase flow. Pergamon Press, Oxford.

Hirofumi, H., Webb, R.L., 1995. Condensation in extruded aluminium tubes, Penn State, Research Report, Showa Aluminum Corporation.

Idelchik, I.E., 1996. Handbook of Hydraulic Resistance, third ed. Begell House, New York. p. 790.

Ishii, M., Mishima, K., 1989. Droplet entrainment correlation in annular two-phase flow. International Journal of Heat and Mass Transfer 32 (10), 1835–1846.

Jeong, S., Cho, E., Kim, H.-K., 2005. Evaporative heat transfer and pressure drop of CO_2 in a microchannel tube. In: Proceedings of the Third International Conference on Microchannels and Minichannels, June 13–15, Toronto, ASME.

Kandlikar, S.G., Grande, W.J., 2003. Evolution of microchannel flow passages – thermohydraulic performance and fabrication technology. Heat Transfer Engineering 24 (1), 3–17.

Kim, M.H., Shin, J.S., Huh, C., Kim, T.J., Seo, K.W., 2003. A study of condensation heat transfer in a single mini-tube and review of Korean micro- and mini-channel studies. In: Proceedings of the First International Conference on Microchannels and Minichannels, Rochester, ASME, New York, pp. 47–58.

Kosky, P.G., Staub, F.W., 1971. Local condensing heat transfer coefficients in the annular flow regime. AIChE Journal 17 (5), 1037–1043.

Koyama, S., Kuwara, K., Nakashita, K,. 2003. Condensation of refrigerant in a multi-port channel. In: Proceedings of the First International Conference on Microchannels and Minichannels, Rochester, ASME, New York, pp. 193–205.

Lopez de Bertodano, M.A., Assad, A., Beus, S., 2001. Experiments for entrainment rate of droplets in the annular flow regime. International Journal of Multiphase Flow 27 (4), 685–699.

Matkovic, M., 2006. Experimental condensation inside minichannels, Doctoral thesis, Università di Padova, p. 209.

Mishima, K., Hibiki, T., 1996. Some characteristics of air–water two-phase flow in small diameter vertical tubes. International Journal of Multiphase Flow 22 (4), 703–712.

Müller-Steinhagen, H., Heck, K., 1986. A simple friction pressure drop correlation for two-phase flow in pipes. Chemical Engineering Progress 20 (6), 297–308.

NIST, National Institute of Standard and Technology, 2002. Refprop Version 7.0, Boulder Colorado.

Paleev, I.I., Filippovich, B.S., 1966. Phenomena of liquid transfer in two-phase dispersed annular flow. International Journal of Heat and Mass Transfer 9 (10), 1089–1093.

Paliwoda, A., 1992. Generalized method of pressure drop calculation across pipe components containing two-phase flow of refrigerants. International Journal of Refrigeration 15 (2), 119–125.

Pan, L., Hanratty, T.J., 2002. Correlation of entrainment for annular flow in horizontal pipes. International Journal of Multiphase Flow 28 (3), 385–408.

Taylor, J.B., Carrano, A.L., Kandlikar, S.G., 2006. Characterization of the effect of surface roughness and texture on fluid flow-past, present, and future. International Journal of Thermal Sciences 45 (10), 962–968.

Wang, Wei-Wen W., Radcliff, T.D., Christensen, R.N., 2002. A condensation heat transfer correlation for millimetre-scale tubing with flow regime transition. Experimental Thermal and Fluid Science 26 (5), 473–485.

Webb, R.L., Ermis, K., 2001. Effect of hydraulic diameter on condensation of R-134a in flat, extruded aluminum tubes. Enhanced Heat Transfer 8 (2), 77–90.

Yan, Y.-Y., Lin, T.-F., 1999. Condensation heat transfer and pressure drop of refrigerant R134a in a small pipe. International Journal of Heat and Mass Transfer 42 (4), 697–708.

Zhang, M., 1998. A new equivalent Reynolds number model for vapor shear-controlled condensation inside smooth and micro-fin tubes. Ph.D. Thesis, The Pennsylvania State University, p. 190.

Zhang, M., Webb, R.L., 2001. Correlation of two-phase friction for refrigerants in small-diameter tubes. Experimental Thermal and Fluid Science 25 (3–4), 131–139.